Journal of Engineering Science and Technology
Vol. 13, No. 3 (2018) 715 - 724

STRUCTURAL CHARACTERISATION AND OPTICAL PROPERTIES OF ALUMINUM-DOPED ZINC OXIDE NANOFIBERS SYNTHESIZED BY ELECTROSPINNING

BAYU SUTANTO[1,2], ZAINAL ARIFIN[1], SUYITNO[1,*]

[1]Department of Mechanical Engineering, Universitas Sebelas Maret, Surakarta, Indonesia
[2]Faculty of Mechanical and Aerospace Engineering, Institut Teknologi Bandung, Indonesia
*Corresponding Author: suyitno@uns.ac.id

Abstract

Nanostructured zinc oxide (ZnO) materials have been of interest for researchers because of their elemental abundance, nontoxicity, and wide range of applications. Furthermore, ZnO characteristics can be tuned *via* doping (e.g. using aluminum (Al)) in order to enhance their properties. In this work, Al-doped ZnO (AZO) nanofibers were synthesized by electrospinning using polyvinyl alcohol (PVA), zinc acetate and aluminum chloride as precursors, then the effect of aluminum doping would be investigated. The nanofibers were characterised by X-ray diffraction (XRD), scanning electron microscopy (SEM), and ultraviolet-visible (UV-Vis) spectroscopy. As a direct band gap material, the optical band gap energy of AZO can be determined by a Tauc plot. The results show that Al doping decreases the crystallite size, nanofiber diameter and band gap energy of ZnO semiconductors. Meanwhile, as the aluminum doping increased above 1 wt%, the crystallite size increased resulting in increased particle size and band gap energy.

Keywords: Zinc Oxide (ZnO), Aluminum doping, Nanofibers, Electrospinning, Band gap energy.

1. Introduction

Zinc oxide (ZnO) is a wurtzite semiconductor with a wide range of applications, such as transparent conductive oxides [1], dye-sensitized solar cells [2-5], thermoelectric [6], and piezoelectric [7, 8]. The morphology and properties of

Nomenclatures

A	Constant for Tauc's relation
c	Velocity of light, 2.998×10^{8} m/s
D	Crystal size, nm
E_g	Optical band gap energy, eV
h	Planck's constant, 6.626×10^{-34} Js
hv	Incident photon energy, eV
k	Scherrer constant, 0.9
v	Frequency (s^{-1})

Greek Symbols

α	Absorption coefficient
β	Full width at half-maximum intensity
λ	Wavelength of the light, nm
θ	Diffraction angle, rad.

Abbreviations

AZO	Aluminum-doped ZnO
FWHM	Full Width at Half-Maximum
MW	Molecular Weight
PVA	Polyvinyl Alcohol
PVP	Polyvinyl Pyrrolidone
SEM	Scanning Electron Microscopy
UV-Vis	Ultraviolet-Visible
XRD	X-ray Diffraction
ZnO	Zinc Oxide

ZnO can be tuned by doping with elements, such as Ga, Al, Sn, In [9, 10]. Aluminum-doped ZnO (AZO) was reported to possess enhanced electrical properties compared to pure ZnO [2, 10]. Furthermore, Al doping was shown to not only improve the electrical properties of ZnO semiconductors, but also to influence the structure and morphology of ZnO nanorods [11].

Recently, several different methods to manufacture ZnO nanomaterials have been proposed, such as sol-gel synthesis [12], inert gas condensation [13], plasma synthesis [14], electrodeposition [15], mechanical alloying [16], and electrospinning [1, 17]. The electrospinning method has been used extensively to fabricate nanofiber structures due to its simplicity, low-cost and morphology control capabilities by simply adjusting process parameters [18, 19].

There are two common vehicles for preparing the precursor solution in electrospinning process, i.e. polyvinyl alcohol (PVA) and polyvinyl pyrrolidone (PVP). PVA and PVP have similar functional group as shown in Fig. 1. PVP are hydrophilic and biodegradable. In contrast, PVA has poor hydrophilicity and low elasticity. Whereas the high elasticity is indispensable to prevent the damage on green fibers before sintering process.

There are, however, only few published reports available on the effect of dopant addition into precursor solutions which made of zinc acetate and PVA on the

morphological, crystallite, optical, and band gap energy properties of ZnO and AZO nanofibers obtained by electrospinning. This research focuses on synthesizing of the precursor solution for ZnO and AZO nanofiber with PVA as a vehicle. This work produced long continuous ZnO and AZO nanofibers up to several hundred of micrometers which suitable for piezoelectric nanogenerator and light scattering layer in dye-sensitized solar cells.

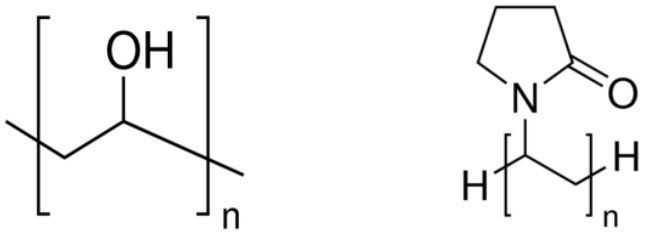

(a) (b)

Fig. 1. Molecular structure of (a) PVA and (b) PVP.

2. Experimental Procedures

2.1. ZnO and AZO nanofibers synthesis

A PVA solution was synthesized by dissolving 2 g polyvinyl alcohol (Merck, MW = 72,000) in 20 mL distilled water (H_2O) for 4 h at 70 ºC. The solution was allowed to left at 30 ºC for 24 h. A detailed description of the synthesis of AZO nanofibers can be found elsewhere [2, 7]. For the zinc acetate solution, 2 g zinc acetate dihydrate ($(CH_3COO)_2Zn{\cdot}2H_2O$, Merck) was dissolved in 8 mL H_2O and stirred for 2 h at 70 ºC. To introduce aluminum, 1, 2, 3, and 4 wt% of aluminum chloride hexahydrate ($AlCl_3{\cdot}6H_2O$, Merck) was mixed with 4 g of the zinc acetate solution and stirred at 70 ºC for 2 h. Homogenization of zinc acetate and zinc acetate/$AlCl_3$ solution was carried out separately with the PVA solution at a weight ratio of 1:4 at 70 ºC for 8 h. The resulting solution was then allowed to left at 30 ºC for 24 h to clear up the foam formed. These precursor solutions were used for the fabrication of undoped (ZnO) and AZO nanofibers.

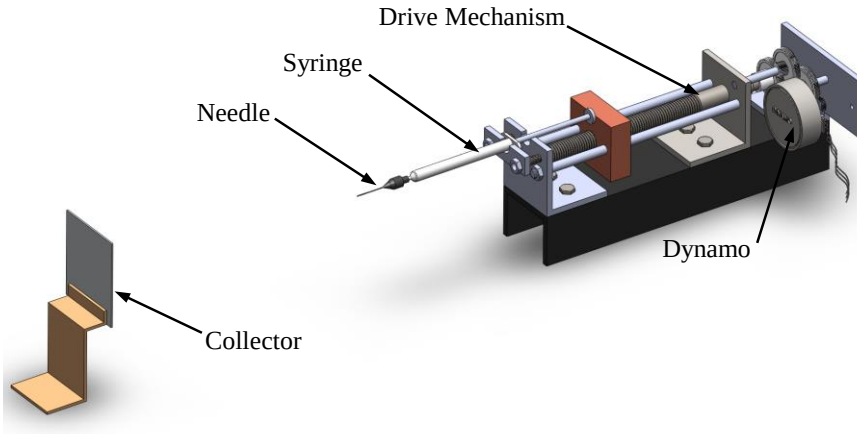

Fig. 2. Electrospinning machine to fabricate AZO nanofibers.

Figure 2 shows a generalized electrospinning set-up to produce nanofiber materials. In a typical procedure, 1 mL precursor solution was transferred into the syringe pump. The needle of the syringe pump was connected to the positive charge of a high-voltage (15 kV) power supply, at a distance of 8 cm horizontally, from the collector plate that was connected to the negative charge. The syringe pump was set to a flow rate of 6 μL/min. The resultant "green fibers" were sintered at 500 ºC for 1 h with heating rate 7 ºC/min, to remove the organic materials and to generate the final ZnO nanofibers. The ZnO nanofibers were subsequent cooled to 50 ºC with cooling rate 1.5 ºC/min.

2.2. Characterisation

The crystallite sizes of the as-prepared ZnO and AZO nanofibers were calculated from XRD measurements. The morphology and nanofiber diameter of the different samples were analyzed by SEM. The optical properties of the AZO samples were measured using UV-Vis spectroscopy in absorbance mode.

3. Results and Discussion

3.1. X-ray diffraction (XRD)

Figure 3 shows the XRD patterns of ZnO and AZO nanofibers, which are in good compatibility with the standard pattern of Zincite (ZnO) (JC-PDF No.36-1451). The main diffraction peaks correspond to the (100), (002), and (101) crystal planes. Surprisingly, the Al-doping process did not change the X-ray diffraction pattern of ZnO semiconductors as no peaks originating from Al or Al_2O_3 (Aluminum Oxide) were visible in these patterns. It can be assumed that Al^{3+} entered the ZnO crystal structure and/or replaced Zn^{2+} because of its ionic radius smaller than Zn^{2+} (0.053 nm and ~0.074 nm respectively) [11].

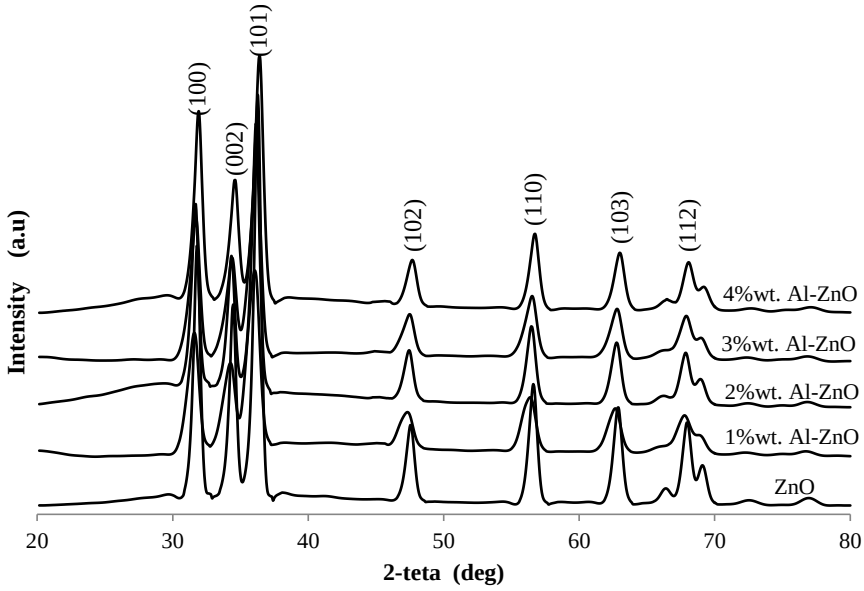

Fig. 3. XRD pattern of various AZO nanofibers.

The highest peak detected in all samples, corresponding to the crystallographic plane (101), can be used to estimate the crystal size of each individual sample by the Scherrer equation in Eq. (1) [20, 21].

$$D = \frac{k.\lambda}{\beta.\cos\theta} \tag{1}$$

where D is the crystal size (nm), λ is the wavelength of the X-ray radiation (Cu/Kα, 0.15406 nm), k is a constant (0.9), θ is the diffraction angle, and β is the full width at half-maximum intensity (FWHM) on the crystallographic plane (101) [2]. Accordingly, the estimated crystallite size of various samples can be seen in Fig. 4.

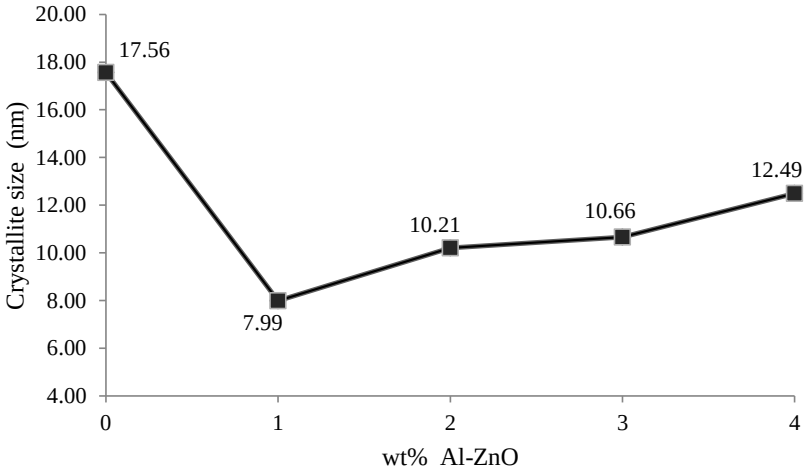

Fig. 4. Crystallite size of various Al-doped ZnO nanofibers.

Figure 4 illustrates that Al doping of ZnO results in a decrease in its crystallite size. This effect was desirable for the preparation of ZnO nanofibers since a smaller crystal size generally induces a decrease in particle size and diameter of the final fibrous product [10]. The smallest crystallite size achieved was 7.99 nm, for the sample containing 1 wt% Al-doped. Further increase of Al doping then increase the crystallite size of ZnO nanofibers. These results consistent with a similar type of crystal structure behavior of ZnO nanofibers with PVP as a vehicle and ZnO nanorods that have been previously reported [10, 11].

3.2. Scanning electron microscopy (SEM)

The structure and morphology of the as-prepared nanofibers is characterised by SEM as shown in Fig. 5. The images clearly indicate that all nanofibers exhibit a cylindrical, branched structure. Table 1 shows the diameter values of the various AZO nanofibers, revealing that the diameter of the ZnO nanofibers also changes with the addition of aluminum. These results showed that the smallest diameter obtained was 85.65 nm for the 1 wt% Al-ZnO sample.

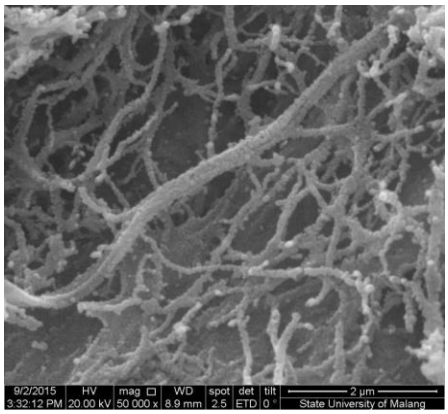

(a) 0 wt% Al-doped

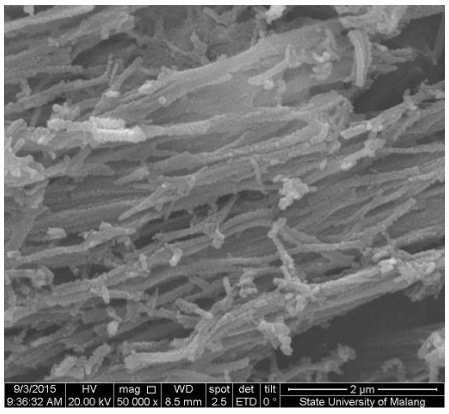

(b) 1 wt% Al-doped

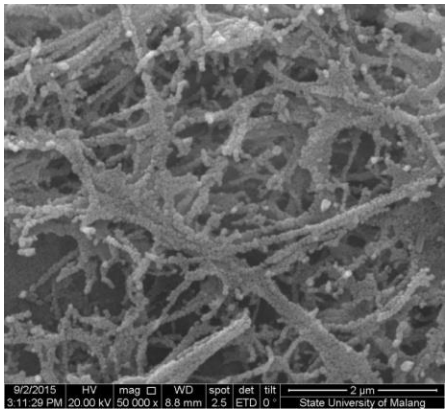

(c) 2 wt% Al-doped

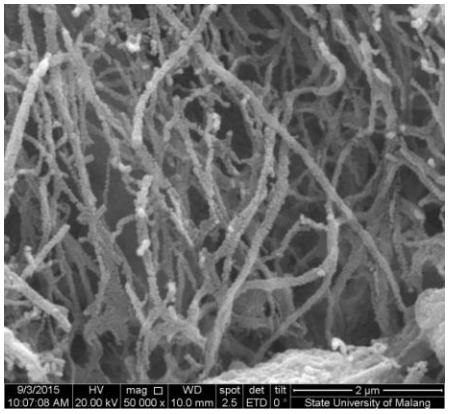

(d) 3 wt% Al-doped

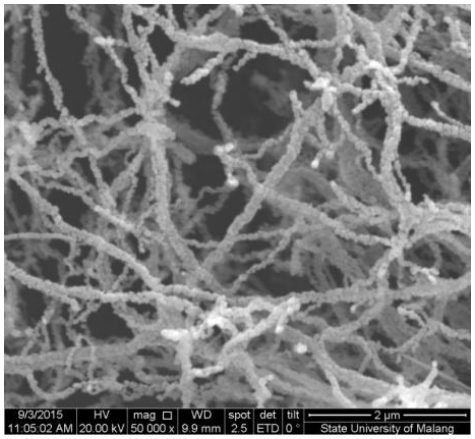

(e) 4 wt% Al-doped

Fig. 5. SEM images of AZO nanofibers doped with the various Al doped.

Table 1. Diameter of various AZO nanofibers.

Al-doped	Minimum (nm)	Maximum (nm)	Mean (nm)	Standard Deviation (nm)
0 wt%	67.59	141.49	107.39	17.52
1 wt%	62.17	114.57	85.65	14.33
2 wt%	49.45	126.20	92.70	16.12
3 wt%	52.05	146.54	99.23	21.31
4 wt%	79.22	161.54	104.84	19.26

Overall, the diameter of the as-prepared ZnO nanofibers decreased with the introduction of Al. This was caused by the presence of Al^{3+} in the precursor solution, which increased electrical conductivity and simultaneously decreased the solution viscosity [10]. The increased solution conductivity resulted in stronger forces of attraction within the electric field of the high-voltage power supply, thereby reducing the obtained fiber diameter due to elongation during the electrospinning process. The result adapted from Ref. [10] shows that the maximum electrical conductivity was obtained at 1.7 at% Al doped ZnO with PVP as a vehicle. PVP is lower in electrical conductivity than PVA. So, the minimum diameter size of ZnO nanofibers for this work was achieved for 1 wt% Al-ZnO sample. The size decreasing of nanofibers will increase the surface area of semiconductors. For electrode application in dye-sensitized solar cell, increasing of surface area will enhance the capability of semiconductor to absorb the dye molecules and increase the output voltage and power of nanogenerator for piezoelectric application.

3.3. Ultraviolet-visible (UV-Vis) spectroscopy

A Rayleigh UV-180 spectrophotometer was used to plot the optical absorption coefficients of the as-prepared AZO nanofibers as a function of the photon energy for wavelengths between 200 and 800 nm as shown in Fig. 6. The band gap energy of AZO nanofibers can be determined by employing the Tauc relation in Eq. (2) [22, 23].

$$(\alpha.h\nu)^2 = A(h\nu - E_g) \quad (2)$$

where α is the absorption coefficient, $h\nu$ is the incident photon energy, A is a constant and E_g is the electronic energy of the optical band gap [24]. The photon energy is determined by h, the Planck's constant (6.626×10^{-34} Js) and ν, the frequency = c/λ, where c is the velocity of light (2.998×10^{8} m/s) and λ is the wavelength of light.

The optical band gap energy (E_g) of AZO samples was determined from the intercepts with the energy axis (x-axis) by extrapolation of linear fit to the $(\alpha\cdot h\nu)^2$ vs. $h\nu$ curve as shown in Fig. 6 [24]. Based on the Tauc plot, the band gap energy of undoped ZnO nanofibers was calculated as 3.52 eV. Furthermore, the band gap energies for 1, 2, 3, and 4 wt% Al-doped ZnO nanofibers were determined to be 3.42, 3.44, 3.48, and 3.50 eV, respectively. This indicates that the incorporation of aluminum into the ZnO structure decreased the band gap energy, which is consistent with a similar type of E_g behavior that has been previously reported for thin film nanostructures synthesized by spray pyrolysis method [23, 25]. The band gap energy of ZnO decrease at the low doping concentration due to the

disturbance of carrier concentration in the conduction band and activation energy level in the nanofiber matrix [10, 23]. After 1 wt% Al doping into ZnO nanofibers, the band gap energy slightly increase with increasing Al concentration. This phenomena is mostly believed to be Burstein-Moss effect. The Burstein-Moss effect is seen as a shift of band gap because of Fermi energy lies in the conduction band for ZnO which is naturally n-type semiconductor. Because of the state below Fermy level in the conduction band is filled, the interband absorption should shift to the higher energy (i.e. a blue shift) [24, 25]. The decreasing of band gap energy in ZnO structure plays an importance role for electrode application such as in dye-sensitized solar cells and piezoelectric nanogenerator. The band gap energy influence the excitation energy of electron from valence band to conduction band [22-26].

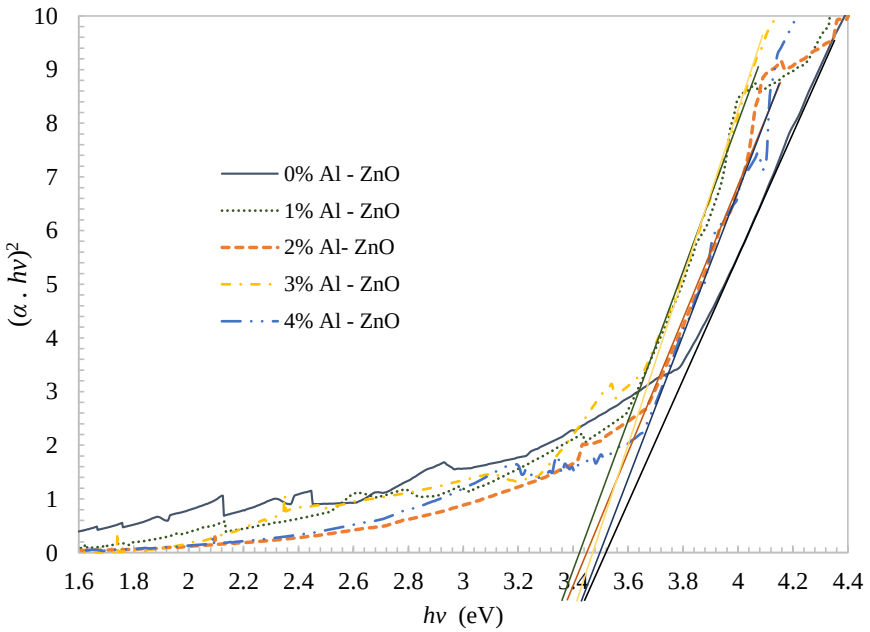

Fig. 6. The $(\alpha \cdot hv)^2$ vs. hv curve of ZnO and AZO nanofibers.

4. Conclusions

The fabrication of aluminum-doped ZnO nanofibers by employing an electrospinning method has been successfully demonstrated. Furthermore, it has been shown that the addition of aluminum dopant decreased the crystallite size, the fiber diameter, and the optical band gap energy of zinc oxide. It was found that the 1 wt% Al-doped ZnO sample exhibited the smallest crystallite size, which consequently resulted in a decrease in diameter of the nanofiber and optical band gap energy of the ZnO semiconductor.

Acknowledgements

The authors acknowledge the Rector of Sebelas Maret University (UNS), LPDP and DP2M DIKTI for the support by research grant No.632/UN27.21/LT/2016, No. 623/UN.27.21/PP/2017, 204/UN27.21/TU/2018, and 2620/UN27.1/PP/ 2017.

The first author is thankful to LPDP (Indonesia Endowment Fund for Education) for the scholarship program No.PRJ-6854/LPDP.3/2016.

References

1. Park, M.; and Han, S.M. (2015). Enhancement in conductivity through Ga, Al dual doping of ZnO nanofibers. *Thin Solid Films*, 590, 307-310.
2. Sutanto, B.; Arifin, Z.; Suyitno; Hadi, S.; Pranoto, L.M.; and Agustia, Y.V. (2016). Enhancement ZnO nanofiber as semiconductor for dye-sensitized solar cells by using Al doped. *AIP Conference Proceedings of Sustainable Energy and Advanced Materials.* Surakarta, Indonesia, 040006.
3. Dou, Y.; Wu, F.; Fang, L.; Liu, G.; Mao, C.; Wan, K.; and Zhou, M. (2016). Enhanced performance of dye-sensitized solar cell using Bi_2Te_3 nanotube/ZnO nanoparticle composite photoanode by the synergistic effect of photovoltaic and thermoelectric conversion. *J. Power Sources*, 307, 181-189.
4. Sakai, N.; Miyasaka, T.; and Murakami, T.N. (2013). Efficiency enhancement of ZnO-based dye-sensitized solar cells by low-temperature $TiCl_4$ treatment and dye optimization. *Physical Chemistry*, 117(21), 10949-10956.
5. Sakai, N.; Usui, R.; and Murakami, T.N. (2013). Optimum particle size of ZnO for dye-sensitized solar cells *Chemistry Letters*, 42(8), 810–812.
6. Cai, K.F.; Müller, E.; Drašar, C.; and Mrotzek, A. (2003). Preparation and thermoelectric properties of Al-doped ZnO ceramics. *Materials Science and Engineering B*, 104(1), 45-48.
7. Suyitno; Purwanto, A.; Hidayat, R.L.L.G.; Sholahudin, I.; Yusuf, M.; Huda, S.; and Arifin, Z. (2014). Fabrication and characterization of zinc oxide-based electrospun nanofibers for mechanical energy harvesting. *Journal of Nanotechnology in Engineering and Medicine*, 5(1), 011002.
8. Suyitno; Sholiehul, H.; Zainal, A.; and Syamsul, H. (2014). Repeatability, reproducibility, and durability of zinc oxide fibre-based nanogenerator synthesized by simple electrospinning machine. *Advanced Science Letters*, 20(10-12), 2299-2303.
9. Norton, D.P.; Heo, Y.W.; Ivill, M.P.; Ip, K.; Pearton, S.J.; Chisholm, M.F.; and Steiner, T. (2004). ZnO: growth, doping & processing. *Materials Today*, 7(6), 34-40.
10. Lotus, A.F.; Kang, Y.C.; Walker, J.I.; Ramsier, R.D.; and Chase, G.G. (2010). Effect of aluminum oxide doping on the structural, electrical, and optical properties of zinc oxide (AOZO) nanofibers synthesized by electrospinning. *Materials Science and Engineering*, 166(1), 61-66.
11. Tao, R.; Tomita, T.; Wong, R.A.; and Waki, K. (2012). Electrochemical and structural analysis of Al-doped ZnO nanorod arrays in dye-sensitized solar cells. *Journal of Power Sources*, 214, 159-165.
12. Astinchap, B.; Moradian, R.; and Nasseri Tekyeh, M. (2016). Investigating the optical properties of synthesized ZnO nanostructures by sol-gel: The role of zinc precursors and annealing time. *Optik - International Journal for Light and Electron Optics*, 127(20), 9871-9877.

13. Uhm, Y.R.; Han, B.S.; Lee, M.K.; Hong, S.J.; and Rhee, C.K. (2007). Synthesis and characterization of nanoparticles of ZnO by levitational gas condensation. *Materials Science and Engineering: A*, 449–451, 813-816.
14. Ma, A.; Rousseau, F.; Donsanti, F.; Lincot, D.; and Morvan, D. (2015). Deposition of ZnO thin films from aqueous solution in a low power plasma reactor. *Surface and Coatings Technology*, 276, 186-194.
15. Yang, J.; Wang, Y.; Kong, J.; Jia, H.; and Wang, Z. (2015). Synthesis of ZnO nanosheets via electrodeposition method and their optical properties, growth mechanism. *Optical Materials*, 46, 179-185.
16. Lin, Y.; Jiang, D.; Lin, F.; Shi, W.; and Ma, X. (2007). Fe-doped ZnO magnetic semiconductor by mechanical alloying. *Journal of Alloys and Compounds*, 436(1–2), 30-33.
17. Anderson, J.; Chris, G.; and Walle, V.d. (2009). Fundamentals of zinc oxide as a semiconductor. *Reports on Progress in Physics*, 72(12), 126501.
18. Li, D.; and Xia, Y. (2004). Electrospinning of nanofibers: reinventing the wheel. *Advanced Materials*, 16(14), 1151-1170.
19. Arifin, Z.; Soeparman, S.; Widhiyanuriyawan, D.; Purwanto, A.; and Dharmanto. (2017). Synthesis, characterisation, and fabrication hollow fibres of Zn-doped TiO_2 for dye-sensitized solar cells. *Journal of Engineering Science & Technology*, 12(5), 1227-1239.
20. Jilani, A.; Iqbal, J.; Rafique, S.; Abdel-wahab, M.S.; Jamil, Y.; and Al-Ghamdi, A.A. (2016). Morphological, optical and X-ray photoelectron chemical state shift investigations of ZnO thin films. *Optik - International Journal for Light and Electron Optics*, 127(16), 6358-6365.
21. Khorsand Zak, A.; Majid, W.H.A.; Ebrahimizadeh Abrishami, M.; Yousefi, R.; and Parvizi, R. (2012). Synthesis, magnetic properties and X-ray analysis of $Zn_{0.97}X_{0.03}O$ nanoparticles (X = Mn, Ni, and Co) using Scherrer and size–strain plot methods. *Solid State Sciences*, 14(4), 488-494.
22. Viezbicke, B.D.; Patel, S.; Davis, B.E.; and Birnie, D.P. (2015). Evaluation of the Tauc method for optical absorption edge determination: ZnO thin films as a model system. *Physical Status Solidi B*, 252(8), 1700–1710.
23. Rahman, M.M.; Khan, M.K.R.; Islam, M.R.; Halim, M.A.; Shahjahan, M.; Hakim, M.A.; Saha, D.K.; and Khan, J.U. (2012). Effect of Al doping on structural, electrical, optical and photoluminescence properties of nano-structural ZnO thin films. *Journal of Materials Science & Technology*, 28(4), 329-335.
24. Hung-Chun Lai, H.; Basheer, T.; Kuznetsov, V.L.; Egdell, R.G.; Jacobs, R.M.J.; Pepper, M.; and Edwards, P.P. (2012). Dopant-induced bandgap shift in Al-doped ZnO thin films prepared by spray pyrolysis. *Journal of Applied Physics*, 112(8), 083708.
25. Shan, F.K.; and Yu, Y.S. (2004). Band gap energy of pure and Al-doped ZnO thin films. *Journal of the European Ceramic Society*, 24(6), 1869-1872.
26. Subagiyo, D.; Thoyib, M.; Suyitno; Hadi, S.; Jamaluddin, A.; and Hidayat, R.L.L.G. (2017). Effect of codoping cobalt and aluminum on enhancing the piezoelectricity properties of fiber-based zinc oxide. *AIP Conference Proceedings of International Conference on Engineering, Science and Nanotechnology*. Surakarta, Indonesia, 030059.